Available online at www.sciencedirect.com
SCIENCE DIRECT®
International Journal of Multiphase Flow 32 (2006) 436–446
International Journal of Multiphase Flow
www.elsevier.com/locate/ijmulflow

Determination of flow sub-regimes in stratified air–water channel flow using LDV spectra

M. Fernandino, T. Ytrehus *

Department of Energy and Process Engineering, Norwegian University of Science and Technology, N-7491 Trondheim, Norway

Received 7 August 2005; received in revised form 19 January 2006

Abstract

In gas–liquid stratified flows, pressure drop and transport across the interface are strongly influenced by the interfacial wave structure, making the determination of interfacial topography in this kind of flows very important. An objective way of characterizing the wave pattern present in the interface is proposed here. The method consists in analysing the spectra of the signal obtained from Laser Doppler Velocimetry (LDV) measurements of fluctuations occurring close to the air-sheared interface. Transitions are defined by the appearance and disappearance of peaks in the frequency spectra. The method was applied to study the transition regimes of a stratified air–water flow in a square-cross section channel. A flow pattern map for air–water channel flow is presented and compared with the maps available from the literature.

Keywords: Channel flow; Interfacial waves; Flow pattern map; Spectral characterization

1. Introduction

Gas–liquid interfaces in stratified flows have been topic of great interest for the last 50 years. Many flow maps for air–water systems can be found in the literature (Mandhane et al., 1974; Taitel and Dukler, 1976; Shoham, 1982; Lin and Hanratty, 1987; Petalas and Aziz, 1998) showing the flow conditions for existence of stratified flows and transitions to other regimes that vary according to pipe diameter, fluid viscosity, and general flow conditions. The maps usually differentiate between a smooth and a wavy stratified sub-regime. However, there are more complex structures that can take place within the wavy sub-regime, namely different interfacial wave patterns, that the mentioned maps do not take into account. The liquid flow structure, pressure drop, liquid hold up, interfacial mass and momentum transfer and the interfacial shear are influenced by the wave pattern occurring at the interface (Andritsos and Hanratty, 1987). In addition, changes in the wave pattern may indicate a probable regime transition. It is therefore of great interest to be able to predict the interfacial structure occurring in a system.

* Corresponding author. Tel.: +47 735 93 557; fax: +47 735 93 491.
E-mail address: tor.ytrehus@ntnu.no (T. Ytrehus).

0301-9322/$ - see front matter
doi:10.1016/j.ijmultiphaseflow.2006.01.003

The transition from stratified smooth to stratified wavy regime has been modeled as the appearance of the first instabilities on the interface. Jeffreys (1925, 1926), assuming that only normal stresses were responsible for the energy transfer from the wind to the liquid flow, suggested a critical velocity based on a sheltering mechanism. Taitel and Dukler (1976), based on the results of Jeffreys (1926) and using some approximations, proposed a similar relation for the critical velocity for wave generation. Cohen and Hanratty (1965) and Craik (1966) used Orr–Sommerfeld stability of horizontal liquid films sheared by a turbulent gas flow to predict the conditions under which waves appear and the factors controlling their growth. Hanratty (1983) and Lin and Hanratty (1986) made use of linear stability theory, the latter including viscous and inertial terms. Funada and Joseph (2001) introduced a new approach to the study of stratified flow stability by using viscous potential flow. These studies describe the conditions for the transition to wavy stratified flow, but do not give any information on the kind of interfacial structure that will take place.

Most of the studies of wave characterization have been conducted for rectangular channels with large aspect ratio (Hanratty and Engen, 1957; Hanratty and Hershman, 1961; Hanratty, 1983; Jurman and McCready, 1989) with application in particular to annular flows. Therefore thin liquid films of the order of millimeters were involved. It is worth noting that they all defined sub-regimes by visual observation.

Some studies regarding stratified flows with moderate liquid film thickness (typically ~2 cm) have been carried out for pipe flows (Andritsos and Hanratty, 1987; Andreussi and Persen, 1987; Espedal, 1998; Spedding and Spence, 1993; Strand, 1993). Andritsos and Hanratty (1987) identified the transition from 2D to 3D waves based on the cross correlation between two wave probes and on the flatness value. The cross correlation value was close to one for 2D waves whereas it was less than unity for 3D waves and decreased for higher gas velocities. More recently Spedding and Spence (1993), used a combination of visual/video observations together with pressure fluctuations characteristics and holdup values for the determination of wave transition.

From all the mentioned studies, flow pattern maps describing the interfacial waves have been proposed, but there are always some discrepancies between them. Not only are the same wave types referred to by different names by different authors, but the transition limits among each sub-regime disagree for some cases as well. One reason may reside in the fact that the wave pattern identification is done rather visually. As mentioned in the previous paragraph, some attempts have been made to describe the wave pattern more objectively. However, the criterion based on the magnitude of the cross correlation value depends on the distance between the two probes. The criterion based on the flatness and skewness values is more difficult to interpret or measure, since higher order moments require more amount of data and thus longer measuring times.

Another way of characterizing the sub-regimes quantitatively is by means of a spectral characterization of the waves. Several authors have shown that different wave patterns present different characteristics on their spectra (Bruno and McCready, 1989; Strand, 1993; Shi and Kocamustafaorgullari, 1994). All these studies used the parallel-wire conductance probe technique (Miya et al., 1971) to track the interface motion and obtain the spectra from the corresponding signal. But even when the frequency characteristics of several types of waves were determined, in either case were these spectral characterizations used to determine pattern transitions.

In this work, spectra from Laser Doppler Velocimetry (LDV) measurements of fluctuations close to the sheared interface are used as a new tool for characterizing wave pattern transitions. The advantage of this method with respect to previous methods (e.g., conductance probes) is that this method is non-intrusive, besides the fact that if LDV is being used to measure velocity profiles as in the study that is being carried out in this laboratory, no additional instrumentation is needed. The experiments are performed for stratified air–water channel flows, involving liquid film thickness of the order of 1–4 cm in a square-section channel. With the transitions observed, a flow pattern map for channel flows and mentioned liquid film heights is presented and compared with existing flow maps from the literature.

2. Description of the experiments

The experiments were carried out in a 9 m long duct, with a square cross-section area of 7 cm × 7 cm. The channel was made of stainless steel and an acrylic transparent section was introduced approximately 6 m from the entrance where the measurements were performed. Fig. 1 shows a schematic diagram of the flow loop.

The study was performed using air and water at atmospheric pressure as working fluids. The air was supplied by the laboratory compressed-air system and was regulated by a manual valve. The water was

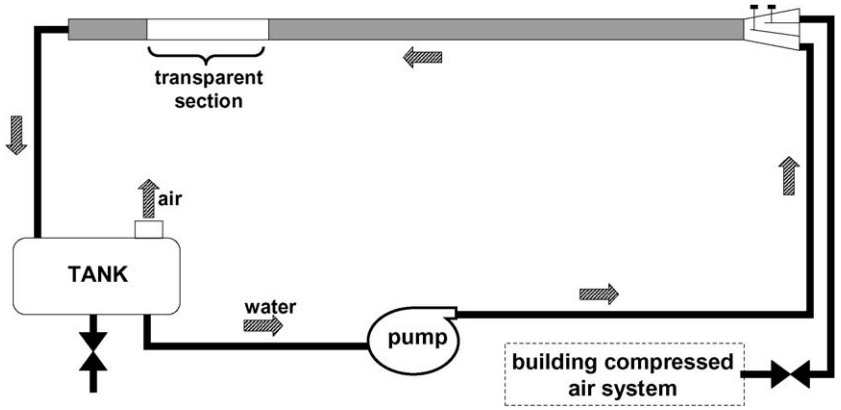

Fig. 1. Experimental facility.

recirculated by a manually regulated screw pump from a tank connected to the outlet of the channel. The water flow rate was monitored by an electromagnetic flow meter and the air flow rate by a mass flow meter operating on a principle of heat transfer along a laminar flow device. Both fluids entered the channel through a square-cross section converging nozzle with two inlets, one above the other (see Fig. 1). The water was introduced through the bottom of the nozzle and the air through the top half.

The pressure drop along the channel and the test section was measured using two dp-cells. A Pt 100 probe placed at the end of the transparent test section was used to record the temperature of the water phase.

Measurements of the liquid velocity and turbulent fluctuations were performed using Laser Doppler Velocimetry (LDV). The laser used was a TSI two-component Argon-Ion laser with wavelengths of 514.4 and 488.0 nm. The laser was mounted on a traverse mechanism capable of shifting position in the vertical and horizontal (streamwise) directions.

The measurements were performed for different combinations of gas and liquid superficial velocities. The liquid superficial velocities (U_{LS}) were 0.037, 0.068, 0.102 and 0.136 m/s, while the gas superficial velocities varied from 0 to 3 m/s. The liquid height was determined by the liquid flow rate, so they could not be varied separately. The laser was aimed at the center plane of the channel as close to the interface as reflections from the interface would allow (approximately 2 mm from the lowest interface level, i.e., from the waves trough).

The frequency spectra were estimated using FIND for Windows, the analysis tool from the acquisition software of the TSI laser used for these experiments. The mentioned software uses the slotting technique (Albrecht et al., 2003) for the estimation of power spectra.

At the same time that a set of measurements was being acquired, a photograph of the flow was taken so as to relate the visually observed interfacial structure with the spectra obtained from the LDV measurements for each flow condition. The photographs were taken with a home digital camera, using shutter times of 1/125 and 1/250. The height and wavelength of the waves were estimated visually from some of the pictures where a ruler was included. These pictures were not included in this report.

3. Results and discussion

3.1. Characterization of wave patterns

Both a visual and then a spectral characterization of the waves observed on the interface during this study will be given here. However, even when a visual difference can be seen between some of the wave patterns, the final characterization will be based on the frequency spectra only, since this last method is more objective than just a visual criterion.

Figs. 2 and 3 show the spectra obtained from the LDV measurements of vertical fluctuations in the liquid phase and the corresponding photographs for the wave patterns observed with $U_{LS} = 0.068$ m/s. There the

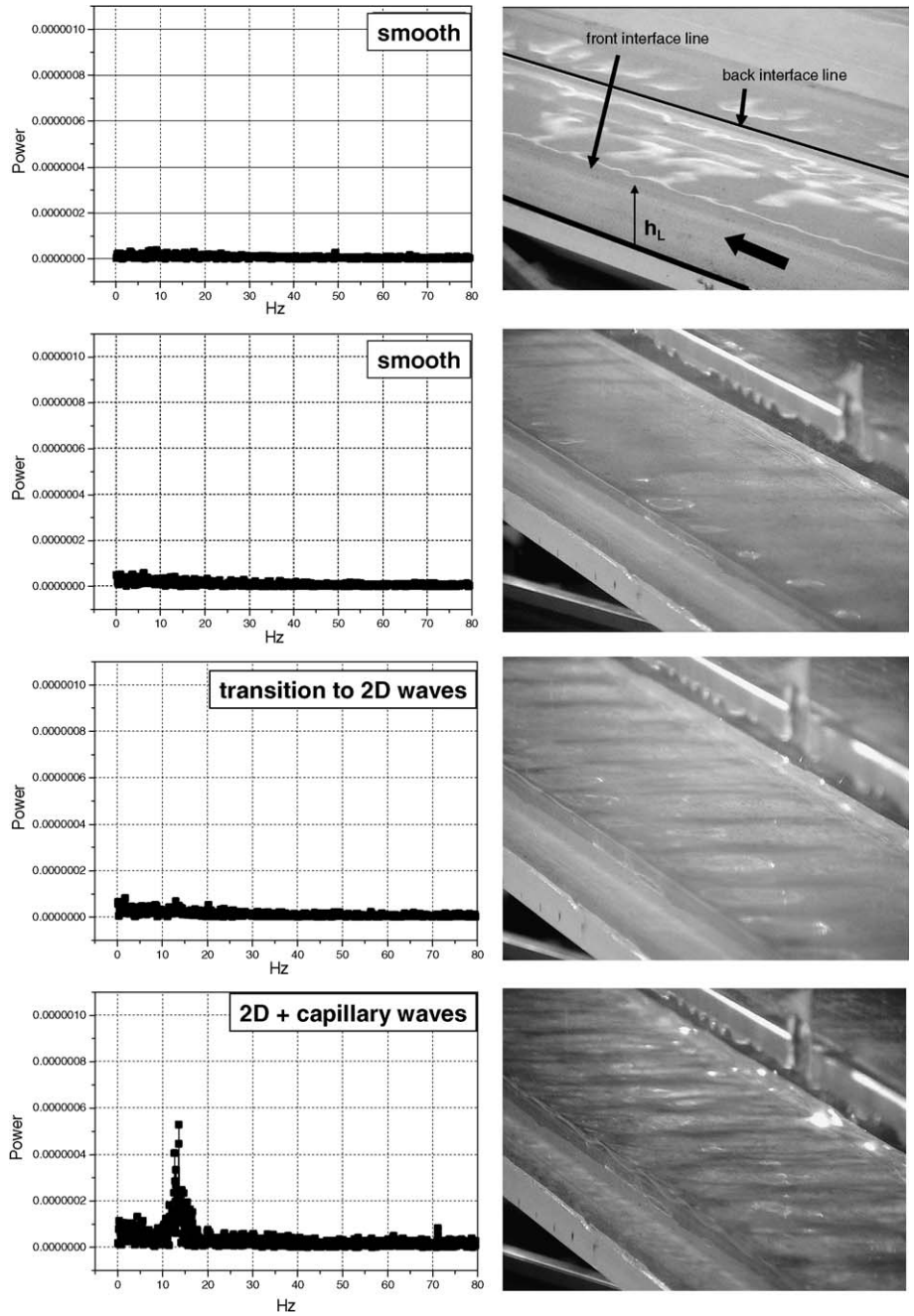

Fig. 2. Wave pattern transitions ($U_{LS} = 0.068$ m/s) for $U_{GS} = 0$ m/s, $U_{GS} = 1.48$ m/s, $U_{GS} = 1.71$ m/s and $U_{GS} = 1.95$ m/s from top to bottom picture (continues in Fig. 3).

power amplitude corresponds to the square of the velocity fluctuations and is thus expressed in units of [m^2/s^2]. These observations are representative of the other three liquid flow rates as well, although the value of the critical velocities for transitions varied for each case.

For sufficiently low gas flow rates, no waves were observed. The reflections that can be seen from the first and second photographs in Fig. 2 were just visually observed by light reflection and the amplitude of the surface topography was not perceived without the light. It is possible to see that in this stratified smooth sub-regime (SS) no frequency peak or dominant frequency appears in the corresponding spectrum. It may

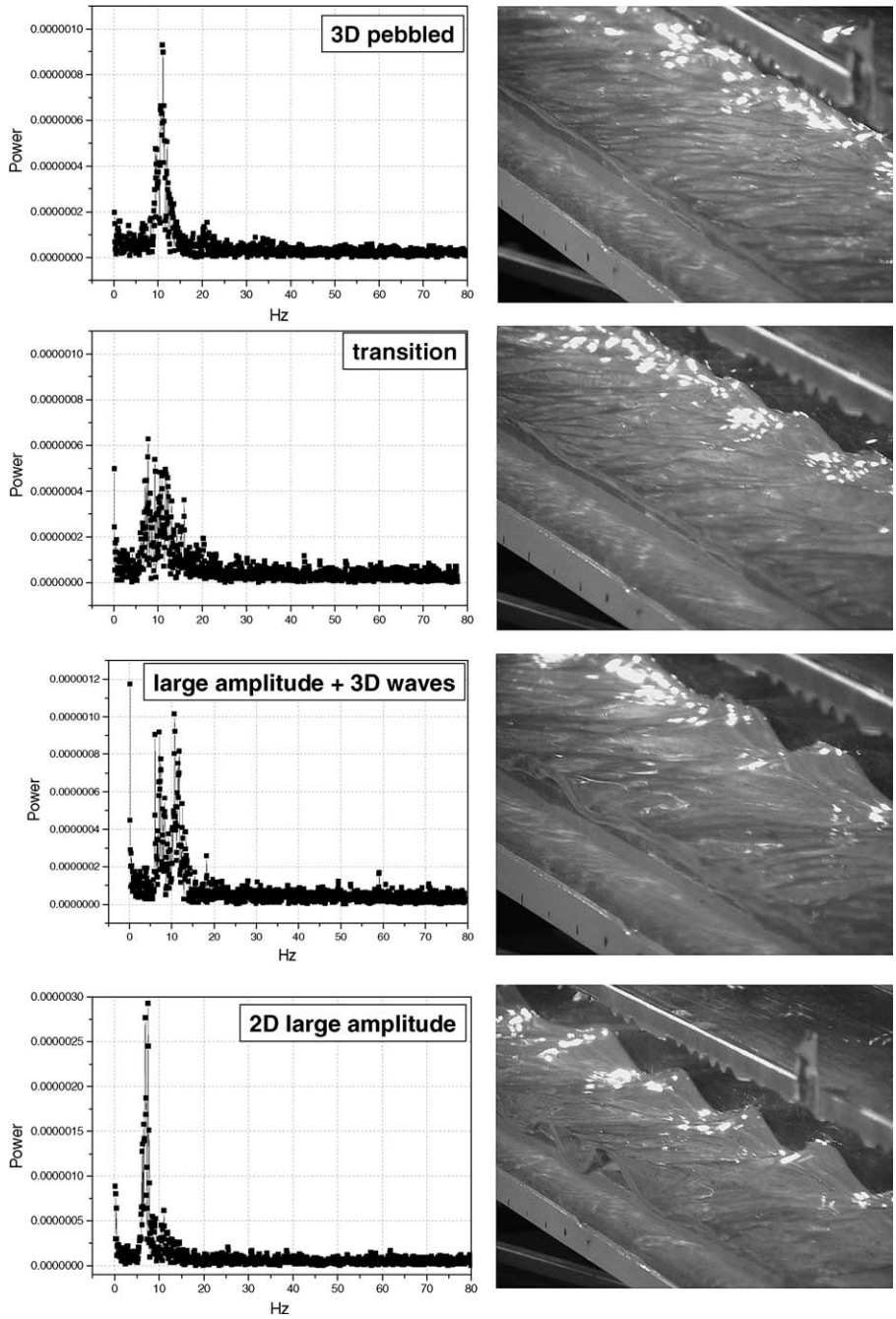

Fig. 3. Wave pattern transitions ($U_{LS} = 0.068$ m/s) for $U_{GS} = 2.40$ m/s, $U_{GS} = 2.55$ m/s, $U_{GS} = 2.65$ m/s and $U_{GS} = 2.88$ m/s from top to bottom picture (continuation from Fig. 2).

be argued that if a pattern similar to the one presented in the second picture of Fig. 2 is observed, then a wavy structure should be defined. However, the corresponding spectrum shows no difference with the smooth interface. This may indicate one limitation of the method, namely that it cannot detect disturbances of very low amplitude that may already be considered waves. The main problem is the fact that this method makes use of vertical fluctuations induced by the interface movement instead of the interface displacement itself. Nevertheless, these fluctuations are induced by this movement, since it is well known that vertical fluctuations are

damped close to the interface if the latter is smooth and that vertical fluctuations intensity increases for a wavy interface as the interface is approached (Rashidi et al., 1992).

As the gas flow rate was increased, two dimensional small-amplitude waves were the first to appear, extending through the whole channel width, with wavelengths from 2 to 4 cm and amplitudes less than 1 mm high. These waves were considered the onset of the stratified wavy regime (SW). At this stage, a first peak started to appear in the spectrum, centered at around 13–14 Hz.

Small capillary waves appeared next superimposed upon the 2D waves as the gas flow rate was further increased (''2D + capillary''). The fourth picture in Fig. 2 shows how the amplitude of the emerging peak at 13–14 Hz was greatly increased. The surface structure became more and more complex with increasing gas velocities, with the appearance also of some pebbled waves and 3D structures with shorter wavelengths (''3D pebbled'') mounted on the 2D small-amplitude waves. All these kinds of perturbations put together gave a general aspect of 3D wave structure on the interface. The mean wave amplitude was somewhat increased from 2 to 3 mm up to around 4 mm. The frequency peak in the spectrum corresponding to these last waves (first picture in Fig. 3) was slightly shifted toward lower frequencies close to 11 Hz. But since there was not any observable change in the nature of the corresponding spectra rather than the slightly continuous shifting to lower frequencies, no distinction between these kinds of waves was made in this work and only one wave pattern was defined during their occurrence. They will be referred to as ''2D small-amplitude + pebbled'' (2D SA + pebbled) waves. This pattern was observed for a wide range of gas velocities. The mentioned shift in frequency can be due to the fact that when the air-flow is increased, the point of initiation of waves moves upstream and the whole wave pattern along the channel is somewhat shifted in that direction. This evolution of wave pattern along the streamwise direction was studied by Fan et al. (1993), who also mentioned a shift of the peak in the wave spectrum from higher to slightly lower frequencies when moving downstream for a fixed combination of air and water flows. They also mentioned that the high frequency waves develop closer to the inlet for the higher gas velocities, but this could not be verified in this work because there was no visual access except in the test section where experiments were performed.

By increasing the air flow still more, a new structure began to form on the interface. This fact was not so easily detected visually, but looking at the spectrum in the second picture from the top of Fig. 3, one can see how the dominating frequency peak of small-amplitude waves broadened and thus marked the emergence of a new structure on the interface.

For slightly higher gas velocities, emerging large-amplitude waves began to appear, coexisting with the small-amplitude 3D waves for a narrow but finite range of gas velocities. The wavelengths were in the order of 4–6 cm. These waves will from now on be called ''3D + LA'', referring to small-amplitude 3D waves together with the first large-amplitude waves. Their amplitude was bigger than the pure 3D waves but still smaller than the large-amplitude waves as defined in this work. It should be noted that Hanratty and Engen (1957) observed the occurrence of roll waves together with squalls, with the former traveling twice as fast as the latter. A similar effect was observed in this study, where bigger waves seemed to travel faster than some smaller ones, catching up with these last ones and creating a new big wave that would catch up with the next small one, and so on. The fact that there were two main waves traveling at different speeds can explain the existence of the two peaks in the frequency spectrum, one around 7 Hz and one around 12 Hz, as shown in the third picture in Fig. 3. This is probably also related to the bifurcation mentioned by Fan et al. (1993).

Higher gas velocities made the 3D waves disappear completely and only large-amplitude 2D waves (2D LA) with a steep front and gradually sloping back remained. These waves were also observed by other authors (Hanratty and Hershman, 1961; Andreussi and Persen, 1987). The observed large-amplitude waves in this study presented wavelengths between 8 and 10 cm, with amplitudes close to 1 cm high. This wave regime was characterized also by a large increase in the gas phase friction factor. The transition from small-amplitude to large-amplitude waves was defined according to the spectrum, when the two peaks joined into one at a lower frequency, as shown in the last picture of Fig. 3. This new peak was centered at around 8 Hz approximately.

These observations show that each different wave pattern presents certain characteristics in its spectrum (such as one or more dominant frequency, for example). Similar things have also been observed by other authors (Bruno and McCready, 1989; Strand, 1993; Shi and Kocamustafaorgullari, 1994). Nevertheless, their approach was usually to trust the visual determination of wave patterns and then to study the characteristic parameters of

each identified pattern such as wavelength, wave height and dominant frequency. Instead, by using this last information as the starting point and relying only on the spectra, visual subjectivity can be avoided.

This spectrum-based method of wave pattern determination clearly avoids any visual subjectivity. For example, it is not obvious how to define the first appearance of waves just visually. Some people may regard just any ripple at all to be an indication of first waves whereas others might expect amplitudes at least greater than 1 mm to consider a disturbance as a wave. This underlying subjectivity can be the reason for discrepancies among empirical flow pattern maps regarding the transition from stratified smooth to stratified wavy regime. In the results presented above, the stratified smooth regime presented a flat spectrum. As the gas flow rate was increased and the first disturbances were present, a clearly dominating frequency was observed in the corresponding spectrum, indicating the onset of some kind of instability at that point. The same holds for the appearance of the first large-amplitude waves. Visually, it was difficult to tell when the new structures appeared. But in this case, the spectrum changed from one dominating frequency to a double-peak spectrum instead. Even if it may be argued that this does not indicate the appearance of large-amplitude waves as defined in this work, this change in the spectrum shape undoubtedly indicates a change in interfacial structure.

The same spectral characterization of wave patterns could be achieved with any other experimental method, such as conductance probes, the parallel wire technique, and any other method able to track the movement of the interface in some way. Since Laser Doppler is at present a widely used technique for the measurement of velocities and turbulence quantities, this technique was chosen for data acquisition and the wave spectra estimation. At the same time that a velocity is being measured, the spectra from that same signal can be used to determine the wave regime present at that moment, without any need of visual subjective determination or the introduction of extra probes to follow the interface displacement.

3.2. Flow pattern map

With the information gathered from the previous section, a flow pattern map describing the observed wave patterns was obtained and is presented in Fig. 4. Transition from stratified smooth (SS) to stratified wavy (SW) is thus defined when the first type of waves appear. As the liquid height increases, the transition from small-amplitude to "3D + large-amplitude" waves (3D + LA) occurs for smaller gas superficial velocities. The 2D large amplitude (LA) waves were not observed for the smallest liquid film. Although the "3D + LA" were visually similar to the "LA" waves observed for the highest gas superficial velocities, these two types could be clearly distinguished from one another from their spectral characteristics.

Fig. 5 shows the here obtained flow pattern map compared with the transitions from smooth to wavy stratified flow predicted by other authors in the literature. It can be seen from this comparison that the transition

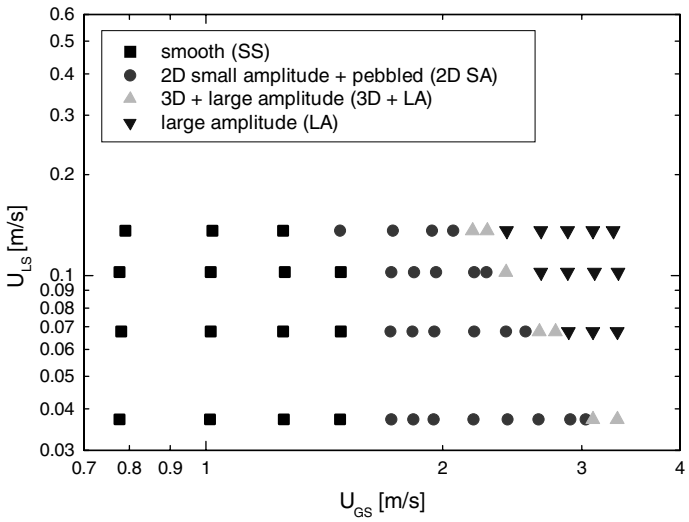

Fig. 4. Flow map for horizontal air–water channel flow, obtained with spectral characterization of waves from LDV measurements.

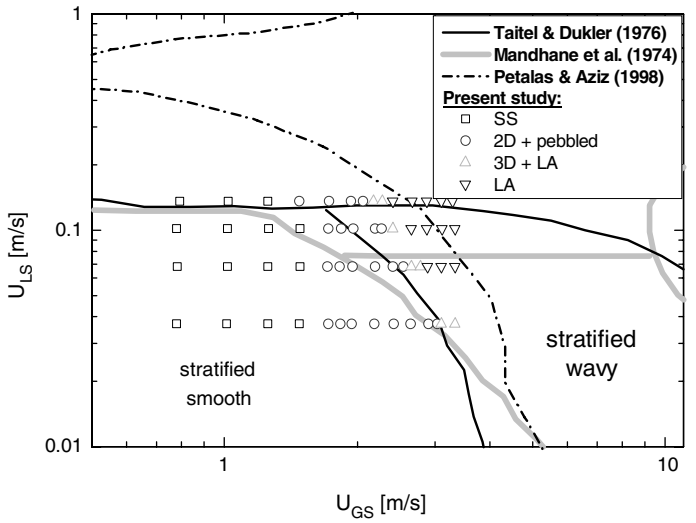

Fig. 5. Comparison of present study results for 7 cm × 7 cm cross section channel flow (SS: stratified smooth; LA: large amplitude) with mechanistic map from Taitel and Dukler (1976), empirical map from Mandhane et al. (1974) for air–water systems in pipes and mechanistic model from Petalas and Aziz (1998) for pipe flows.

defined in this work as transition from smooth to stratified wavy is close to the one predicted by Mandhane et al. (1974) and the mechanistic model from Taitel and Dukler (1976), but it happens for slightly smaller gas superficial velocities. Actually, the transition to wavy stratified flow proposed by Taitel and Dukler (1976) is closer to the initiation of 3D irregular waves observed in this work ("3D + LA"). The model proposed by Petalas and Aziz (1998) shows a gas velocity corresponding to this transition that is high above the one found in this study. The reason may be that the model from Petalas and Aziz (1998) used empirical relationships obtained from a flow data base of pipe flow measurements. Wall and interfacial friction factors were correlated according to these data. The fact that the channel data seems to be higher than the pipe flow data has also been recognized by other authors (Funada and Joseph, 2001).

Fig. 6 shows the flow map obtained in this study for wave pattern transitions as compared to the one obtained by Andritsos and Hanratty (1987) for 9.53 cm diameter pipe flow. The discrepancy between both

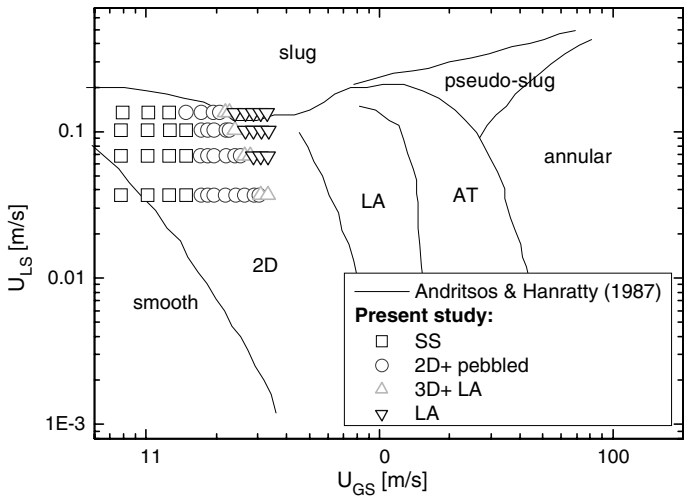

Fig. 6. Flow map from Andritsos and Hanratty (1987) for pipe diameter 9.53 cm (LA: large amplitude; AT: atomization) compared with results from present study for 7 cm × 7 cm cross-section channel flow (SS: stratified smooth; LA: large amplitude).

maps is expected since it is not possible to compare results obtained from pipe flows directly with results coming from channel flows when dealing with regime transitions. Different phenomena take place in each case. Contrary to channel flows, in stratified gas–liquid pipe flow the liquid height is not constant over the flow cross section, and wave patterns and pressure drops are therefore not the same as in a channel. Furthermore, secondary currents that are different from the ones encountered in channel flows take place, giving rise to different wall- and interfacial shear distributions along the pipe.

No comparisons were possible with the flow pattern maps for channel flows from Hanratty and Engen (1957) and Jurman and McCready (1989) since the liquid height in their study was much smaller than the one used in this study and no reasonable match between the flow maps was possible.

3.3. Dominant frequency

As mentioned by Bruno and McCready (1989), wave spectra contain information about the phenomena of wave growth, dissipation and energy transfer. These basic processes define the dynamic energy balance taking place in the system. In principle, interaction between all the harmonics exists in a spectrum of waves generated by gas shear (Bruno and McCready, 1989). The gas flow feeds energy into the fastest growing modes, which in turn provide an energy source for all other waves. Most part of the energy is transfered upward in frequency to shorter-wavelength waves, which dissipate this energy by internal viscous effects. Some resonance effects can also allow transfer of energy from higher to lower frequency waves. But since interaction rates are strongly dependent on the amplitude of the participating waves, the dominant interaction takes place between the fundamental mode (largest amplitude) and the first harmonic. This interaction determines the dominating frequency peak observed in the spectra.

Fig. 7 shows how the dominant characteristic frequency for each wave pattern varies as the pattern changes for increasing air superficial velocity and air mean velocity.

From Fig. 7(a) it can be observed that the same qualitative behavior is present for the four different liquid heights considered here. Only one dominant frequency is present corresponding to the first small-amplitude waves to appear. In all four cases, when large amplitude waves start to form, two frequencies characterize the spectra. This means that the energy coming from the gas is fed primarily into two distinct modes, defining two type of waves which coexist during a finite range of gas velocities. This dual peak in the spectrum corresponds to the appearance of the first large amplitude waves, indicating the transition from small- to large-amplitude interfacial waves. For a higher gas flow rate, only one smaller frequency survives. This decrease in the dominant frequency may be attributed to the coalescence of large amplitude waves to form larger waves.

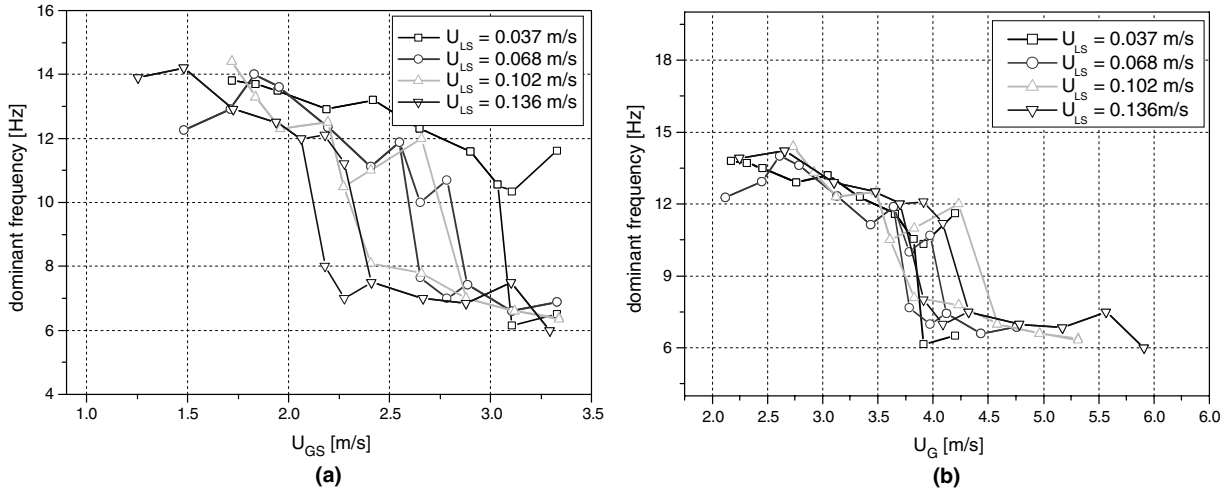

Fig. 7. Dominant frequency in each wave pattern spectrum as a function of: (a) the gas superficial velocity U_{GS} and (b) the mean gas velocity U_G.

If the dominant frequency is plotted against the mean gas velocity U_G Fig. 7(b), it is seen that the transition from small- to large-amplitude waves occurs practically for the same mean gas velocity for the four different liquid heights. This may suggests that, irrespective of the liquid height (at least for the range involved in this work), the initiation of large amplitude waves is triggered when the gas kinetic energy is greater than a critical value $E_G^{crit} = 1/2\rho_G U_{G,crit}^2$.

Clearly, two different mechanisms of energy transfer occur above and below the critical value of gas kinetic energy, which may explain the observations of Andritsos and Hanratty (1987) about the interfacial instabilities caused by air flow over a liquid film. Below $U_{G,crit}$ 2D small-amplitude waves exist which are associated with pressure variations in the gas phase in phase with the wave slope. Above $U_{G,crit}$ large-amplitude waves are formed which are associated with pressure variations in the gas phase in phase with the wave height. However, no mention of the liquid height dependence was made by the latter authors. Some dependence of a possible critical gas energy value on the liquid height is expected for different liquid viscosities and surface tension.

4. Conclusions

In this work two main issues were discussed. The first one was the determination of different wave regimes in stratified channel flows based on an objective method. The method consists in analysing the spectra coming from LDV measurements of the vertical velocity fluctuations close to the air-sheared interface. Changes in the wave characteristics were evident by the appearance or disappearance of peaks in the corresponding spectrum. In this way, even when some visual differences may have been appreciated, the transitions from one sub-regime to another was objectively determined by the differences found in each spectrum.

The second issue presented here was the construction of a flow pattern map for horizontal stratified air–water channel flow using the information gathered with the previous method. The flow pattern map was compared to other maps found in the literature. But since some of them included empirical data coming from pipe flow experiments, the agreement with them was not so good, apart from the fact that there could also be some discrepancies in the visual determination of the wave patterns. Some flow pattern maps for channel flows were found but for liquid layer heights that were too small compared with the ones used in the present study.

Acknowledgements

This work was made possible thanks to the financial support of the Norwegian Research Council through CARPET Strategic University Program.

References

Albrecht, H.E., Borys, M., Damaschke, N., Tropea, C., 2003. Laser Doppler and phase Doppler measurement techniques. Experimental Fluid Mechanics. Springer.

Andreussi, P., Persen, L.N., 1987. Stratified gas–liquid flow in downwardly inclined pipes. Int. J. Multiphase Flow 13, 565–575.

Andritsos, N., Hanratty, T.J., 1987. Interfacial instabilities for horizontal gas–liquid flows in pipelines. Int. J. Multiphase Flow 13, 583–603.

Bruno, K., McCready, M.J., 1989. Study of the processes which control the interfacial wave spectrum in separated gas–liquid flows. Int. J. Multiphase Flow 15, 531–552.

Cohen, L.S., Hanratty, T.J., 1965. Generation of waves in the cocurrent flow of air and a liquid. AIChE.J. 11, 138–144.

Craik, A.D.D., 1966. Wind-generated waves in thin liquid films. J. Fluid Mech. 26, 369–392.

Espedal, M., 1998. An experimental study of stratified two-phase pipe flow at small inclinations. PhD thesis, NTNU, Norway.

Fan, Z., Lusseyran, F., Hanratty, T.J., 1993. Initiation of slugs in horizontal gas–liquid flows. AIChE J. 39, 1741–1753.

Funada, T., Joseph, D.D., 2001. Viscous potential flow analysis of Kelvin–Helmholtz instability in a channel. J. Fluid Mech. 445, 263–283.

Hanratty, T.J., Hershman, A., 1961. Initiation of roll waves. AIChE J. 7, 488–497.

Hanratty, T.J., 1983. Interfacial instabilities caused by air flow over a thin liquid layer. Waves on Fluid Interfaces. Academic Press, New York.

Hanratty, T.J., Engen, J.M., 1957. Interaction between a turbulent air stream and a moving water surface. AIChE J. 3, 299–304.

Jeffreys, H., 1925. On the formation of water waves by wind. Proc. R. Soc. A 107, 189–201.

Jeffreys, H., 1926. On the formation of water waves by wind. Proc. R. Soc. A 110, 241–268.

Jurman, L.A., McCready, M.J., 1989. Study of waves on thin liquid films sheared by turbulent gas flows. Phys. Fluids A 1, 522–536.

Lin, P.Y., Hanratty, T.J., 1986. Prediction of the initiation of slugs with linear stability theory. Int. J. Multiphase Flow 12, 79–98.

Lin, P.Y., Hanratty, T.J., 1987. Effect of pipe diameter on flow patterns for air–water flow in horizontal pipes. Int. J. Multiphase Flow 13, 549–563.

Mandhane, J.M., Gregory, G.A., Aziz, K., 1974. A flow pattern map for gas–liquid flow in horizontal pipes. Int. J. Multiphase Flow 1, 537–553.

Miya, M., Woodmansee, D.E., Hanratty, T.J., 1971. A model for roll waves in gas–liquid flow. Chem. Eng. Sci. 26, 1915–1931.

Petalas, N., Aziz, K., 1998. A mechanistic model for multiphase flow in pipes. In: 49th Annual Technical Meeting of the Petroleum Society of the Canadian Institute of Mining, Metallurgy and Petroleum, June 8–10, Alberta, Canada.

Rashidi, M., Hetsroni, G., Banerjee, S., 1992. Wave-turbulence interaction in free-surface channel flows. Phys. Fluids A 4, 2727–2737.

Shi, J., Kocamustafaorgullari, G., 1994. Interfacial measurements in horizontal stratified flow patterns. Nucl. Eng. Des. 149, 81–96.

Shoham, O., 1982. Flow pattern transitions and characterization in gas–liquid two phase flow in inclined pipes. PhD thesis, Tel-Aviv University, Ramat-Aviv, Israel.

Spedding, P.L., Spence, D.R., 1993. Flow regimes in two-phase gas–liquid flow. Int. J. Multiphase Flow 19, 245–280.

Strand, Ø., 1993. An experimental investigation of stratified two-phase flow in horizontal pipes. PhD thesis, University of Oslo, Norway.

Taitel, Y., Dukler, A.E., 1976. A model for predicting flow regime transitions in horizontal and near-horizontal gas–liquid flow. AIChE J. 22, 47–55.